OXFORD
SOT | Society of Toxicology
academic.oup.com/toxsci

Toxicological Sciences, 2023, **193(1)**, 31–47
https://doi.org/10.1093/toxsci/kfad027
Advance Access Publication Date: March 13, 2023
Research article

Adolescent exposure to low-dose Δ^9-tetrahydrocannabinol depletes the ovarian reserve in female mice

Jinhwan Lim,[1,2] Hye-Lim Lee,[3] Julie Nguyen,[4] Joyce Shin,[1,4] Samantha Getze,[4] Caitlin Quach,[4] Erica Squire,[3] Kwang-Mook Jung,[3] Stephen V. Mahler,[5] Ken Mackie,[6] Daniele Piomelli,[3] Ulrike Luderer [1,2,4,*]

[1]Department of Environmental and Occupational Health, University of California Irvine, Irvine, California 92697, USA
[2]Dept. of Medicine, University of California Irvine, Irvine, California 92697, USA
[3]Department of Anatomy and Neurobiology, University of California Irvine, Irvine, California 92697, USA
[4]Department of Developmental and Cell Biology, University of California Irvine, Irvine, California 92697, USA
[5]Department of Neurobiology and Behavior, University of California Irvine, Irvine, California 92697, USA
[6]Department of Psychological and Brain Sciences, Indiana University, Bloomington, Indiana 47405, USA

*To whom correspondence should be addressed at Center for Occupational and Environmental Health, 856 Health Sciences Rd (Quad), Suite 3200 Zot 1830, Irvine, CA 92697, USA. E-mail: uluderer@uci.edu

Abstract

Cannabis use by adolescents is widespread, but its effects on the ovaries remain largely unknown. Δ^9-tetrahydrocannabinol (THC) exerts its pharmacological effects by activating, and in some conditions hijacking, cannabinoid receptors (CBRs). We hypothesized that adolescent exposure to THC affects ovarian function in adulthood. Peripubertal female C57BL/6N mice were given THC (5 mg/kg) or its vehicle, once daily by intraperitoneal injection. Some mice received THC from postnatal day (PND) 30–33 and their ovaries were harvested PND34; other mice received THC from PND30–43, and their ovaries were harvested PND70. Adolescent treatment with THC depleted ovarian primordial follicle numbers by 50% at PND70, 4 weeks after the last dose. The treatment produced primordial follicle activation, which persisted until PND70. THC administration also caused DNA damage in primary follicles and increased PUMA protein expression in oocytes of primordial and primary follicles. Both CB1R and CB2R were expressed in oocytes and theca cells of ovarian follicles. Enzymes involved in the formation (N-acylphosphatidylethanolamine phospholipase D) or deactivation (fatty acid amide hydrolase) of the endocannabinoid anandamide were expressed in granulosa cells of ovarian follicles and interstitial cells. Levels of mRNA for CBR1 were significantly increased in ovaries after adolescent THC exposure, and upregulation persisted for at least 4 weeks. Our results support that adolescent exposure to THC may cause aberrant activation of the ovarian endocannabinoid system in female mice, resulting in substantial loss of ovarian reserve in adulthood. Relevance of these findings to women who frequently used cannabis during adolescence warrants investigation.

Keywords: Δ^9-tetrahydrocannabinol; cannabis; cannabinoid receptors; ovary; premature ovarian failure; ovarian follicle

Cannabis is, along with alcohol and tobacco, one of the most commonly used psychoactive drugs worldwide. According to the 2020 Monitoring the Future Study survey, its use typically starts in early to mid-teenage years and gradually increases throughout adolescence. In 2021, 10% of American 8th graders, 22% of 10th graders, and 39% of 12th graders reported using cannabis at least once (Miech *et al.*, 2021), with an estimated 48.2 million people aged 12 or older and 3.3 million adolescents aged 12–17 in 2019 using it (SAMSHA, 2020). Cannabis use may cause a wide range of adverse health effects on the brain and body, and adolescents who consume it are four to seven times more likely to develop cannabis use disorder (dependence and withdrawal) than adults (Miech *et al.*, 2021). It is important, therefore, to elucidate how cannabis consumption during adolescence might affect health in adulthood, particularly the reproductive health of women, which is still poorly understood.

Δ^9-Tetrahydrocannabinol (THC) is the primary psychoactive ingredient of cannabis (Fezza *et al.*, 2014; Gaoni and Mechoulam, 1964; Iversen, 2003; Piomelli, 2003). Its pharmacological target is the endocannabinoid system (ECS), a signaling complex that serves a vast array of modulatory functions in mammalian physiology. The ECS is comprised of cell-surface cannabinoid (CB) receptors (CB1R and CB2R, encoded in mice by the *Cnr1* and *Cnr2* genes), two lipid-derived ligands—arachidonoylethanolamide (anandamide, AEA) and 2-arachidonoyl-*sn*-glycerol (2-AG), and intracellular proteins involved in the formation, transport and deactivation of such molecules (Jung and Piomelli, 2022). THC directly binds and activates both isoforms of cannabinoid receptor (CBR) to produce its pharmacological effects (Devane *et al.*, 1988; Matsuda *et al.*, 1990; Munro *et al.*, 1993). CB1R mediates most of the central and peripheral actions of THC, while CB2R contributes to other effects including regulation of pain and immunity (Freund *et al.*, 2003; Kano *et al.*, 2009; Lu and Mackie, 2021; Mackie, 2005). The hijacking of these receptors by THC may cause aberrant activation of CBR-mediated signaling, especially at high doses, which contrasts with highly regulated activation by its endogenous ligands, AEA and 2-AG (Devane *et al.*, 1992; Di Marzo *et al.*, 1994; Jung and Piomelli, 2022; Lu and Mackie, 2021;

Mechoulam *et al.*, 1995; Stella *et al.*, 1997; Sugiura *et al.*, 1995). The levels of these endocannabinoid molecules are tightly regulated, both temporally and spatially, through a set of enzymes and transporters that cooperate to ensure that CBRs are engaged only when and where their activation is needed (Jung and Piomelli, 2022; Piomelli *et al.*, 2007).

Biosynthesis of anandamide starts with the transfer of an arachidonate group from the *sn*-1 position of 1,2-diarachidonoyl-phosphatidylcholine to the free amino group of phosphatidylethanolamine (PE), which generates the anandamide precursor *N*-arachidonoyl-PE (Di Marzo *et al.*, 1994); Reviewed in (Piomelli and Mabou Tagne, 2022). This reaction is catalyzed by the calcium-dependent *N*-acyl transferase activity of cytosolic type-ε phospholipase A_2, PLA2G4. Hydrolytic cleavage of membrane-bound *N*-arachidonoyl-PE by a phospholipase D (NAPE-PLD) releases anandamide, which diffuses out of the cell and into the external milieu. Anandamide is deactivated through a two-step process in which the compound is first internalized by cells by an as-yet-uncharacterized facilitated-diffusion mechanism, followed by intracellular hydrolysis catalyzed by the serine amidase fatty acid amide hydrolase (FAAH) (Piomelli and Mabou Tagne, 2022). Biosynthesis of endocannabinoids is summarized in Figure 1.

AEA and 2-AG have been reported to inhibit the development of cultured mouse 2-cell embryos to the blastocyst stage in a CB1R-dependent manner (Paria *et al.*, 1998). Furthermore, *in vivo* infusion of THC in the presence of cytochrome P450 inhibitors, but not THC alone, inhibited blastocyst implantation in mice, and a CB1R antagonist prevented this effect (Paria *et al.*, 1998). By contrast, AEA may accelerate trophoblast differentiation of cultured mouse blastocysts (Wang *et al.*, 1999). These studies suggest developmental stage-specific roles for the ECS in embryonic development. It has been reported that CB1R and CB2R are present in granulosa, theca and luteal cells of human (El-Talatini *et al.*, 2009) and rat (Bagavandoss and Grimshaw, 2010) ovaries.

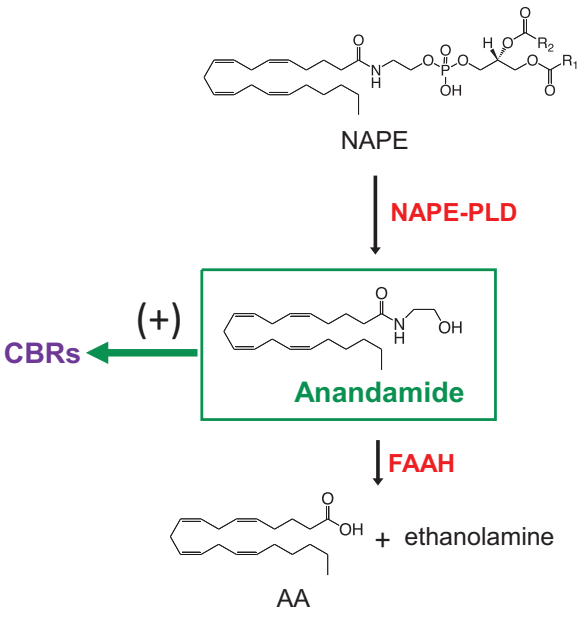

Figure 1. Enzymatic steps for anandamide formation and degradation. The key enzymatic step for anandamide biosynthesis is the hydrolysis of the phospholipid precursor, *N*-arachidonoyl-phosphatidylethanolamine (NAPE), catalyzed by a selective phospholipase D (NAPE-PLD). Once formed, anandamide binds and activates either type1 or 2 CB receptors (CBRs) and is degraded intracellularly by the serine amidase, fatty acid amide hydrolase (FAAH) to arachidonic acid (AA) and ethanolamine.

Enzymes that synthesize and metabolize endocannabinoids have also been detected in human and rat ovaries, indicating the ECS is active during folliculogenesis in the ovary (Brents, 2016; El-Talatini *et al.*, 2009). Experimental studies have demonstrated that exposure to CBR agonists suppresses the release of gonadotropin-releasing hormone, follicle-stimulating hormone (FSH), and luteinizing hormone (LH) in rodents and primates (Almirez *et al.*, 1983; Asch *et al.*, 1995, 1981; Smith *et al.*, 1979a,b). THC exposure also resulted in poor oocyte quality and embryonic mortality due to arrested development at the zygote stage or implantation failure (Paria *et al.*, 1998). In a controlled human study, smoking one cannabis cigarette acutely decreased serum LH concentrations during the luteal phase of the menstrual cycle, but not during the follicular phase (Mendelson *et al.*, 1986). These findings collectively suggest that a finely tuned ECS is required for normal pregnancy and ovarian functions. However, the possible roles of the ECS in ovarian steroidogenesis and folliculogenesis have not been satisfactorily studied and, in particular, the long-term effects of ECS perturbation on the ovaries remain unknown.

FSH acts on granulosa cells to stimulate estradiol synthesis and secretion, while LH acts on theca cells to stimulate synthesis of androgens, which are converted to estradiol in the granulosa cells (Gore-Langton and Armstrong, 1994; Miller and Auchus, 2011). Steroidogenic acute regulatory protein (StAR) is responsible for the rate-limiting step in steroidogenesis, transfer of cholesterol to the inner mitochondrial membrane, where cholesterol is converted to pregnenolone by cholesterol side-chain cleavage enzyme, CYP11A1 (Jefcoate *et al.*, 1992). Pregnenolone is converted to progesterone by 3β-hydroxysteroid dehydrogenase2 (HSD3B2), while cytochrome P450 17A1 (CYP17A1) regulates androgen synthesis in theca cells by catalyzing the conversion of progesterone into androstenedione. Then, 17β-hydroxysteroid dehydrogenase3 (HSD17B3) catalyzes the conversion of androstenedione to testosterone, and aromatase (CYP19A1) catalyzes the conversion of androstenedione and testosterone into estrone and estradiol, respectively, in granulosa cells (Miller and Auchus, 2011). Ovarian toxicant-induced disruption of steroidogenesis has been identified in animal models (Hannon *et al.*, 2015; Lee *et al.*, 2013; Wójtowicz *et al.*, 2007). However, whether THC affects ovarian steroid biosynthetic machinery has not yet been elucidated.

The size of the primordial follicle pool is the key determinant of reproductive lifespan in females (Lei and Spradling, 2013; Reddy *et al.*, 2010). Exhaustion of such pool coincides with menopause, which normally occurs in humans at age 50 ± 4 years (van Noord *et al.*, 1997). The ovarian reserve gradually declines as primordial follicles are activated to grow by paracrine signals independent of gonadotropin stimulation and mature into gonadotropin-dependent growing follicles (Juengel and McNatty, 2005). Although genetic mutations, as well as treatment with antineoplastic agents and ionizing radiation, are known causes of premature depletion of the ovarian reserve, the proximal causes of early onset of ovarian senescence are in most cases unknown (Greene *et al.*, 2014; Nelson, 2009; Rebar, 2005). There are two main mechanisms through which exposure to chemicals or ionizing radiation may cause early depletion of the ovarian reserve, namely, induction of apoptotic death of primordial follicles and accelerated activation of primordial follicles (Kalich-Philosoph *et al.*, 2013; Luderer, 2014; Spears *et al.*, 2019). Whether THC affects ovarian folliculogenesis and steroidogenesis and if so, the mechanisms underlying such effects, has not been investigated. In the present report, we tested the hypothesis that THC

exposure in adolescence might activate quiescent primordial follicles and/or initiate cell death pathways in follicles, resulting in premature depletion of the ovarian reserve.

Materials and methods

Animals

C57BL/6N mice (Charles River) were housed in an American Association for the Accreditation of Laboratory Animal Care-accredited facility, with free access to water and chow (Harlan Teklad, 2919) on a 12:12 h light-dark cycle, and were acclimated to the vivarium for 7 days prior to treatment. Temperature was maintained at 69–75°F. The experimental protocols were carried out in accordance with the Guide for the Care and Use of Laboratory Animals and were approved by the Institutional Animal Care and Use Committee at the University of California Irvine.

THC administration

Immature female mice were treated with intraperitoneal (IP) injections of THC (5 mg/kg, once daily) or vehicle (5% Tween 80 in 0.9% saline) for 14 days from PND 30 to PND 43 (sub-chronic study, $n = 10$/treatment) or for 4 days from PND 30 to PND 33 (acute study, $n = 10$/treatment). Ovaries were harvested at PND 70 (sub-chronic study, to determine the effects of adolescent exposure on ovarian endpoints in young adulthood) or PND 34 (to determine the acute ovarian effects of adolescent THC exposure), 24 h after the last injection. We selected the IP route for two reasons: (1) is the route most frequently used in rodent studies and (2) it offers a realistic compromise between technical feasibility, reproducibility, and translational relevance. While smoking and, to a lesser extent, "vaping" are the most common means of cannabis consumption in people, animal studies generally rely on IP injection, which is practical and reproducible and elicits in rodents pharmacokinetic and pharmacodynamic responses that are comparable to those seen in cannabis smokers. For example, previous studies have shown that IP injection results in substantial and reproducible tissue concentrations of Δ^9-THC in adolescent and adult mice and rats of both sexes and produces peaks in plasma concentrations that are quantitatively comparable to those observed in adult nonmedical cannabis smokers (Huestis, 2007; Torrens *et al.*, 2020, 2023). Specifically, 5 mg/kg IP resulted in plasma peak THC concentrations in adult male mice (198 ± 20 ng/ml) very similar to peak plasma concentrations in adult men (162 ± 34 ng/ml) after smoking one cannabis cigarette containing about 34 mg of THC (Huestis and Cone, 2004; Torrens *et al.*, 2020). Moreover, this dosage elicits only modest pharmacological effects in adolescent male mice (Lee *et al.*, 2022; Torrens *et al.*, 2020) and thus offers a human-relevant model for frequent low-intensity THC exposure.

Follicle counting

Mice were humanely euthanized using CO_2 asphyxiation. PND 34 and PND 70 ovaries were harvested and one ovary per mouse was randomly selected and immediately fixed in Bouin's solution at 4°C overnight, washed in 50% ethanol three times, and stored in 70% ethanol until embedding in glycolmethacrylate resin (Technovit 8100; Heraeus Kulzer GmBH, Wehrheim, Germany). Embedded ovaries were sectioned at 20 μm and stained with hematoxylin and eosin. Stereological methods were used to obtain unbiased estimates of ovarian follicle numbers (Lim *et al.*, 2022; Myers *et al.*, 2004, 2015). Ovarian follicles were counted blind to treatment group using Stereo Investigator software (MBF Bioscience) with an Olympus BX40 light microscope equipped with 10× Plan and 40× PlanApo N340 objectives, a joystick controller for a motorized XY stage (Ludl Electronic Products), and an Optronics MicroFire digital camera. The fractionator/optical dissector method was used to estimate primordial and primary follicle numbers by counting follicles in a defined fraction of the whole ovary (Myers *et al.*, 2004). Three levels of sampling were used to determine the estimated number of primordial and primary follicles in the ovary. First, every fifth section of the ovary was counted. For the second level of sampling, 15 620 μm^2 (125 μm × 125 μm) counting frames were superimposed onto the sections in sampling grids that were subdivided into 40 000 μm^2 (200 μm × 200 μm) squares. Follicles were counted if the oocyte fell within the counting frame and/or touched the inclusion boundaries and did not touch the exclusion boundaries. Lastly, the optical dissector height was set to 10 μm with guard zones on the top and the bottom of the section to account for irregularities of the sections. After processing the sections were 18.5 μm thick on average, and only the middle 10 μm of the sections were counted. By multiplying the raw counts by the reciprocals of the counting fractions, the number of follicles in the entire ovary was estimated. Secondary and antral follicles and corpora lutea were followed through every section to avoid counting any of these large structures more than once. Follicles were classified as primordial (a single layer of flattened granulosa cells with no more than one cuboidal granulosa cell), primary (a single layer with two or more cuboidal granulosa cells), secondary (more than one layer of granulosa cells with no antrum), or antral (multiple layers of granulosa cells with antrum) follicles. Atretic follicles were identified as previously described (Desmeules and Devine, 2006; Hirshfield, 1988; Lim *et al.*, 2013).

Immunostaining and immunofluorescence assays

Ovaries from PND 34 and PND 70 female mice that received 5.0 mg/kg THC or vehicle once daily PND 30 to PND 33 or PND 30 to PND 43, respectively, were immediately fixed in 4% paraformaldehyde in PBS at 4°C overnight, cryoprotected in 30% sucrose in PBS, embedded in optimal cutting temperature compound, cryosectioned at 7 μm and stored at −80°C until use. Immunofluorescence staining was performed to localize key components of the ECS (CB1R, CB2R, NAPE-PLD, and FAAH) and to counterstain granulosa cells of follicles (FOXL2) in the mouse ovary. Immunohistochemical staining was used to detect DNA damage (γH2AX), apoptosis (PUMA, cleaved caspase 3), and activation of primordial follicles (Ki67) in the mouse ovary.

For immunofluorescence, sections were pretreated in 10 mM citric acid for 15 min at 95°C, blocked in PBS-Triton X-100 solution with 5% normal serum and 1% BSA or with 5% normal donkey serum for 1 h, and incubated with primary antibodies—rabbit anti-CB1R or anti-CB2R (1:100; raised in the laboratory of Dr. Ken Mackie, Indiana University Bloomington) (Bagavandoss and Grimshaw, 2010), rabbit anti-NAPE-PLD (1:100, HPA024338; Sigma Aldrich, St. Louis, Missouri), rabbit anti-FAAH (1:100, HPA007425; Sigma Aldrich), goat anti-FOXL2 (1:200, NB100-1277; Novus Biologicals), rabbit anti-StAR (1:200, No. 203193; Abcam) – at 4°C overnight. After washing, the primary antibodies were detected with corresponding fluorophore-conjugated secondary antibodies (donkey anti-rabbit Alexa Fluora 488 [A21206; Invitrogen] and donkey anti-goat Alexa Fluora 633 [A21082; Invitrogen]) for 1 h at room temperature. Sections were treated with ReadyProbe tissue autofluorescence quenching (R37630; ThermoFisher) for 5 min and mounted in Prolong glass antifade mountant (P36980;

ThermoFisher). Images of fluorescently labeled ovarian follicles were generated and processed using a Leica SP8 microscope and the Bitplane Imaris imaging software (v. 9.8.0). Image processing settings from each channel were adjusted for optimal signal intensity and applied identically to all the images obtained from the same experiment.

For immunohistochemistry, sections were thawed and heated for 15 min in a 10 mM citrate buffer (pH 6.0). The primary antibodies—rabbit anti-γH2AX (1:200, No. 9718; Cell Signaling), rabbit anti-PUMA (1:200, No. 9643; Abcam), rabbit anti-cleaved caspase 3 (1:100, No. 9661; Cell Signaling), rabbit anti-Ki67 (1:500, No. 15580; Abcam)—were detected using biotinylated goat anti-rabbit secondary antibodies in 5% normal goat serum and avidin-biotin-peroxidase complex (Vectastain Elite ABC kit; Vector Laboratories, Burlingame, California). Peroxidase activity was visualized using 3,3′-diaminobenzidine as substrate. Sections were counterstained with hematoxylin. The following negative controls were included in every experiment: secondary antibody without primary antibody; primary antibody without secondary antibody; and primary antibody replaced by rabbit or goat IgG, as appropriate for the primary antibody, with secondary antibody. Both negative and positive follicles for each marker were counted by an investigator blind to experimental group and quantities expressed as fractions were used for statistical analyses. The numbers of Ki67, cleaved caspase-3, PUMA, and γ H2AX-positive and -negative follicles or oocytes were counted in one section per slide for 2 or 3 slides per mouse per endpoint using an Olympus BX-60 microscope. The percentages of positive primordial and primary follicles (containing one or more positive granulosa cells per cross-section or containing positive oocytes) and secondary and antral follicles (containing three or more positive granulosa cells per cross-section or containing positive oocytes) were calculated and used for data presentation and analysis.

RNA isolation

Total RNA was extracted from freshly harvested PND 34 and PND 70 mice ovaries using TRIzol reagent and purified with the PureLink RNA Mini Kit (Thermo Fisher Scientific, Waltham) as directed by the supplier. Prior to purification, samples were rendered genomic DNA free by passing the isolated RNA extract through a gDNA eliminator spin column (Qiagen, Germantown). RNA concentration and purity were determined using the NanoDrop 2000/2000-c spectrophotometer (Thermo Fisher Scientific). cDNA was synthesized using 2 μg of total RNA as input for the High-Capacity cDNA RT Kit with Rnase Inhibitor (Applied BioSystems, Foster City) with a final reaction volume of 20 μl. Following the reaction, the samples were diluted to a final volume of 100 μl.

Quantitative real-time PCR

First-strand cDNA was amplified using TaqMan Universal PCR Master Mix (Thermo Fisher Scientific) following the manufacturer's instructions. Primers and fluorogenic probes were purchased from Applied Biosystems (TaqMan Gene Expression Assays, Foster City, California) and are listed in Table 1. Quantitative real-time reverse transcriptase PCRs (qRT-PCRs) were performed in 96-well plates using CFX96 Real-Time System (Bio-Rad). The thermal cycling conditions were as follows: initial denaturation set at 95°C for 10 min, followed by 45 cycles at 95°C for 30 s followed by 55°C for 60 s. The Bestkeeper software was used to determine the expression stability and the geometric mean of the housekeeping genes (*Actb*, *Hprt*, and *Gapdh*). The expression of each target gene was quantified relative to that of the geometric mean of the housekeeping genes. ΔCt values were calculated and fold change over vehicle control were calculated by the $2^{-\Delta\Delta Ct}$ method (Livak and Schmittgen, 2001).

Table 1. List of validated TaqMan qRT-PCR probes used in the study

Gene Target	Assay ID (Thermo Fisher Scientific)
Hprt	Mm00446968_m1
Actin	Mm00607939_s1
Gapdh	Mm99999915_g1
Cnr1	Mm01212171_s1
Cnr2	Mm02620087_s1
Faah	Mm00515684_m1
Nape-pld	Mm00724596_m1
Cyp17a1	Mm00484040_m1
Hsd3b2	Mm00462685_m1
Star	Mm00441558_m1
Cyp19a1	Mm4453320_m1

Statistical analysis

All values are presented as mean ± SEM in figures. We used Student's *t* test to assess the significance of the difference between experimental groups using SPSS 25.0 (IBM Software). Quantities expressed as fractions were subjected to arcsine square root transformation followed by Student's *t* test or were analyzed by nonparametric Mann-Whitney test.

Results

Effects of adolescent THC exposure on follicle counts in ovaries of PND 34 and PND 70 mice

To evaluate in a quantitative manner the lasting effects of THC exposure on the ovarian reserve, we counted follicles in ovaries of female PND 34 (24 h after the last THC dose) and PND 70 mice (4 weeks after the last THC dose). In THC-treated PND 34 ovaries, the number of follicles of all follicle types did not differ from controls (Supplementary Figure 1). In PND 70 ovaries, however, the measurements revealed statistically significant declines of 37% in the total number of follicles of all stages ($p = .012$, Figure 2A–C) and of 50% in primordial follicles ($p = 0.003$; Figure 2D) in THC-treated mice. Primary and secondary follicle numbers were not significantly affected by THC (Figure 2E and F). By contrast, significant decreases in the numbers of healthy antral follicles ($p = 0.013$; Figure 2G) and corpora lutea ($p = 0.025$; Figure 2H) were observed in THC-treated mice relative to controls. The numbers of atretic antral follicles did not differ between groups (9.6 ± 2.0 in controls and 8.8 ± 1.1 in THC). There were no or very few atretic primordial, primary, or secondary follicles observed in either group (data not shown).

Effects of adolescent THC exposure on primordial follicle activation

Since, as seen above, adolescent THC exposure produced accelerated depletion of the ovarian follicle pool, we examined whether this effect might be mediated via accelerated activation of primordial follicles into the growing pool. This hypothesis was supported by a shift in the percentages of primordial and primary follicles in the THC-treated group compared to the control group. In the control group, 52% of all the healthy follicles were primordial and 40% were primary, while in the THC group 44% were primordial and 46% were primary ($p = 0.07$ and 0.09 for the effect of THC on primordial and primary follicle percentages, respectively, by Mann-Whitney test, Supplementary Figure 2). A controlled

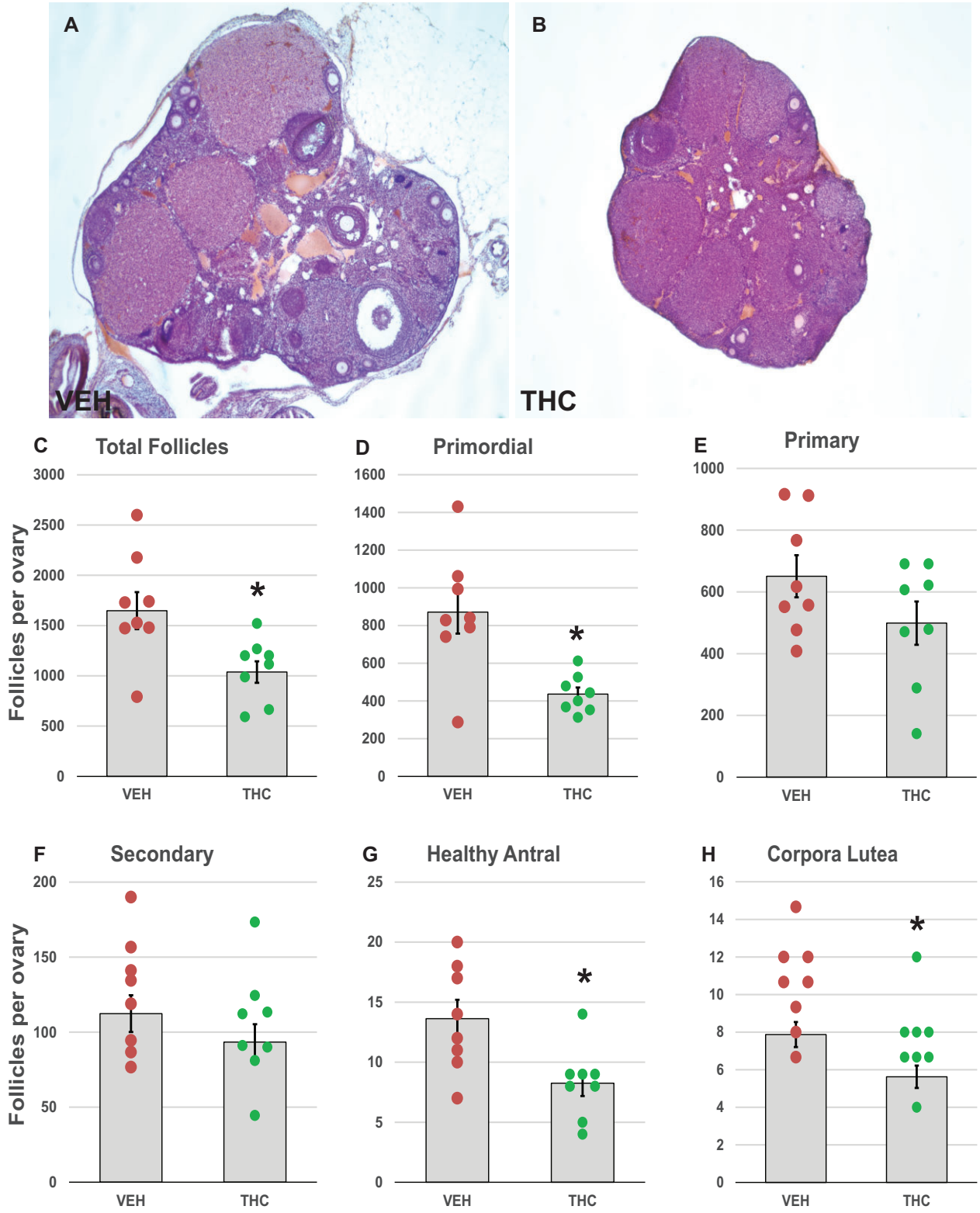

Figure 2. Adolescent THC exposure depletes ovarian follicles: 1-month-old female mice were exposed to THC (5 mg/kg, IP) or vehicle (5% Tween 80 in 0.9% saline) for 2 weeks (PND 30–43) and were euthanized at PND 70 for enumeration of ovarian follicles as described in Materials and Methods. Representative images of cross-sections of hematoxylin and eosin-stained vehicle- (A) and THC-exposed (B) PND 70 ovaries. Graphs show the means ± SEM number of follicles per ovary; dots show values for individual mice. Total number of follicles at all developmental stages (C) and primordial follicle number (D) were significantly decreased in THC-treated mice compared to vehicle controls. No statistically significant differences in primary (E) or secondary (F) follicle numbers were observed between THC-treated and control mice. Healthy antral follicle (G) and corpus luteum numbers (H) were significantly decreased in THC-treated mice compared to vehicle controls. *$p < .05$, t test THC versus vehicle. $N = 8$/group.

number of quiescent primordial follicles is steadily recruited into the growing pool via paracrine signals from surrounding follicles (Zheng *et al.*, 2012). Granulosa cells in activated primordial follicles begin to proliferate. Excessive and continued activation of primordial follicles can lead to accelerated depletion of the ovarian reserve and development of premature ovarian failure (Reddy *et al.*, 2008, 2009).

To test whether the decreases in primordial follicle numbers in THC-treated PND 70 mice could be due to accelerated recruitment of follicles into the growing pool, we performed immunostaining for Ki67, a specific marker of mitosis (Scholzen and Gerdes, 2000), to identify activated follicles based on granulosa cell proliferation. The average percentage of primordial follicles with Ki67-positive granulosa cells was below 3.1% in both PND 34 and PND 70 mice and was not significantly changed by THC treatment (Figure 3). In contrast, the percentage of primary follicles with Ki67-positive granulosa cells was significantly higher in ovaries from PND 34 ($p = .027$; Figure 3C) and PND 70 ($p = .013$; Figure 3D) mice treated with THC, respectively, than in ovaries from mice treated with vehicle. This is consistent with accelerated recruitment of primordial follicles because our counting rubric grouped transitional follicles (follicles with a mix of fusiform and cuboidal granulosa cells) with primary follicles. Moreover, the results show that increased follicle activation persisted for at least 4 weeks after the last THC dose. As expected, all secondary and antral follicles had Ki67-positive granulosa cells irrespective of experimental group (data not shown).

Effects of adolescent THC exposure on ovarian DNA damage and apoptosis

Next, we asked whether treatment with THC might trigger follicle death via DNA damage and subsequent activation of (pro)apoptotic proteins. Initiation and progression of apoptosis were evaluated by immunostaining for γH2AX (Figure 4A and B), a marker of DNA double-strand breaks (Kinner *et al.*, 2008; Riches *et al.*, 2008), PUMA (Figure 5A and B), a pro-apoptotic upstream regulator of caspase-mediated cell death in the mitochondrial apoptotic pathway (Myers *et al.*, 2014; Nguyen *et al.*, 2018), and cleaved caspase 3 (Figure 6A and B), the active form of caspase 3, the so-called executioner caspase (Fenwick and Hurst, 2002). In THC-treated PND 34 mice, percentages of primary follicles with γH2AX-positive oocytes significantly increased compared to the control group ($p = .042$; Figure 4C). Increased DNA damage was not observed in PND 70 ovaries (Figure 4D). We also noted significant increases in the percentages of primordial ($p = .048$) and primary ($p = .012$) follicles with PUMA-positive oocytes in the THC-exposed PND 34 mice compared to the controls (Figure 5C), but not in PND 70 ovaries (Figure 5D), which suggests that increasing DNA damage induced the activation of PUMA. Caspase 3 is activated by either the intrinsic or extrinsic apoptotic pathway, and its activation leads to apoptotic chromatin condensation and DNA fragmentation in the granulosa cells of ovarian follicles (Fenwick and Hurst, 2002). The increased percentage of secondary follicles with activated caspase-3-positive granulosa cells in the PND 34 THC ovaries approached significance ($p = .098$; Figure 6C). No activated caspase 3-positive primordial or primary follicles were detected in the PND 34 and PND 70 ovaries regardless of treatment group.

Immunochemical localization of CB1R, CB2R, FAAH, and NAPE-PLD

To assess whether THC exerts its effects via interaction with the ECS in the ovary, we localized CB1R and CB2R along with the anandamide-metabolizing enzymes NAPE-PLD and FAAH by immunohistochemistry in vehicle or THC-treated mouse ovaries (Figure 7 and Supplementary Figure 3). Immunoreactive CB1R was primarily found in oocytes of primordial, primary, secondary, and antral follicles, the theca cells of growing antral follicles, and the ovarian surface epithelium (OSE) (Figure 7A–C). CB1R was also distinctly localized to mural granulosa and theca cells in preovulatory follicles and corpora lutea (Supplementary Figure 3). CB2R was primarily observed in the interstitial cells and the theca cells of antral follicles. CB2R was also expressed in the oocytes of all follicle types in a similar manner as CB1R (Figure 7D). FAAH immunostaining overlapped with CB1R and was observed in oocytes of primordial, primary, secondary and antral follicles (Figure 7E). FAAH was also strongly expressed in granulosa and theca cells of antral follicles. Like CB2R, NAPE-PLD localized to the theca cells of antral follicles and interstitial cells; however, NAPE-PLD immunoreactivity was absent from oocytes of the ovarian follicles (Figure 7F). Localization and signal intensity of endocannabinoid components in the mouse ovary are summarized in Table 2.

Transcription of CBRs, AEA-metabolizing enzymes, and steroidogenic enzymes in the ovary

We performed qRT-PCR to quantify transcript levels for the genes encoding CB1R and CB2R (*Cnr1* and *Cnr2*, respectively; Figure 8A and B), and AEA-metabolizing enzymes (*Faah* and *Nape-pld*; Figure 8C and D) in PND 34 and PND 70 ovaries. In THC-treated mice, the ovarian levels of *Cnr1* mRNA were significantly increased at PND 34 compared to aged-matched vehicle controls ($p = 0.033$). Elevated *Cnr1* levels persisted at least until PND 70 ($p = 0.032$). Unlike *Cnr1*, ovarian transcription of *Cnr2*, *Faah*, and *Nape-pld* was not affected by THC treatment in PND 34 mice. In PND 70 mice, however, the THC-treated group showed significantly lower expression of *Faah* mRNA compared to control mice ($p = .002$).

We also examined the expression levels of steroidogenic acute regulatory protein (*Star*; Figure 8E) and steroidogenic enzymes (*Hsd3b2*, *Cyp17a1*, and *Cyp19a1*; Figure 8F–H) in PND 34 and PND 70 ovaries. *Star* was significantly downregulated in THC-treated PND 70 ovaries compared to the vehicle group ($p = .022$); however, the expression of *Star* mRNA did not differ between the control and THC-treated groups in the PND 34 ovaries. The expression levels of *Hsd3b2*, *Cyp17a1*, and *Cyp19a1* in the THC-treated mice also showed no difference compared to the control group in PND 34 mice. Because *Cyp17a1* and *Cyp19a1* mRNA expressions vary considerably with estrous cycle stage (LaVoie, 2017; Stocco, 2008), and the PND 70 mice were euthanized without regard to estrous cycle stage, only PND 34 data are shown for those transcripts. To further investigate the potential effect of THC on the rate-limiting step in steroidogenesis—namely, transport of cholesterol into the mitochondria—we localized StAR protein immunofluorescence. StAR immunoreactivity was observed in oocytes of developing follicles and in theca cells of the large antral follicles (Supplementary Figure 4), locations in which CB1R and CB2R expressions were also observed.

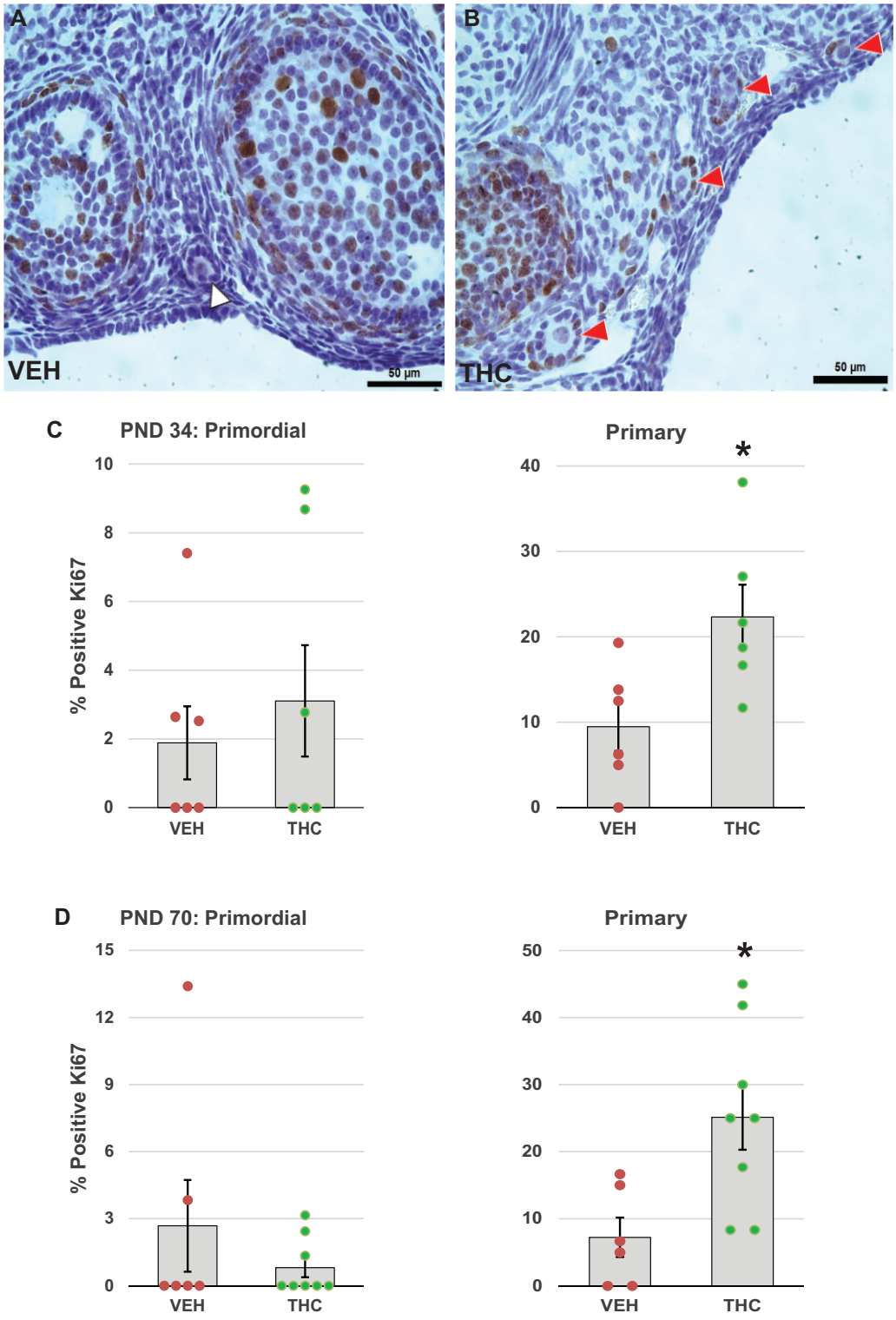

Figure 3. Adolescent THC exposure increases activation of primordial ovarian follicles. One-month-old female mice were exposed to THC (5 mg/kg, IP) or vehicle (5% Tween 80 in 0.9% saline) for 4 days (PND 30–33) or 14 days (PND 30–43) and ovaries were harvested at PND 34 (24 h after the last injection) or PND 70 (4 weeks after the last injection), respectively. PND 34 and PND 70 ovaries were processed for immunostaining for the proliferation protein Ki67 as detailed in Materials and Methods. Representative images show (A) Ki67-negative follicles in vehicle control ovary (white arrowhead) or (B) Ki67-positive follicles with brown stained granulosa cell nuclei in THC ovary (red arrowheads). The graphs show the means ± SEM percentages of Ki67-positive primordial and primary follicles in PND 34 (C) and PND 70 (D) ovaries; dots show values for individual mice. Administration of THC significantly increased the percentage of primary follicles with Ki67-positive granulosa cells. *$p < .05$, t test THC versus vehicle. $N = 6–8$/group. Scale bars, 50 µm.

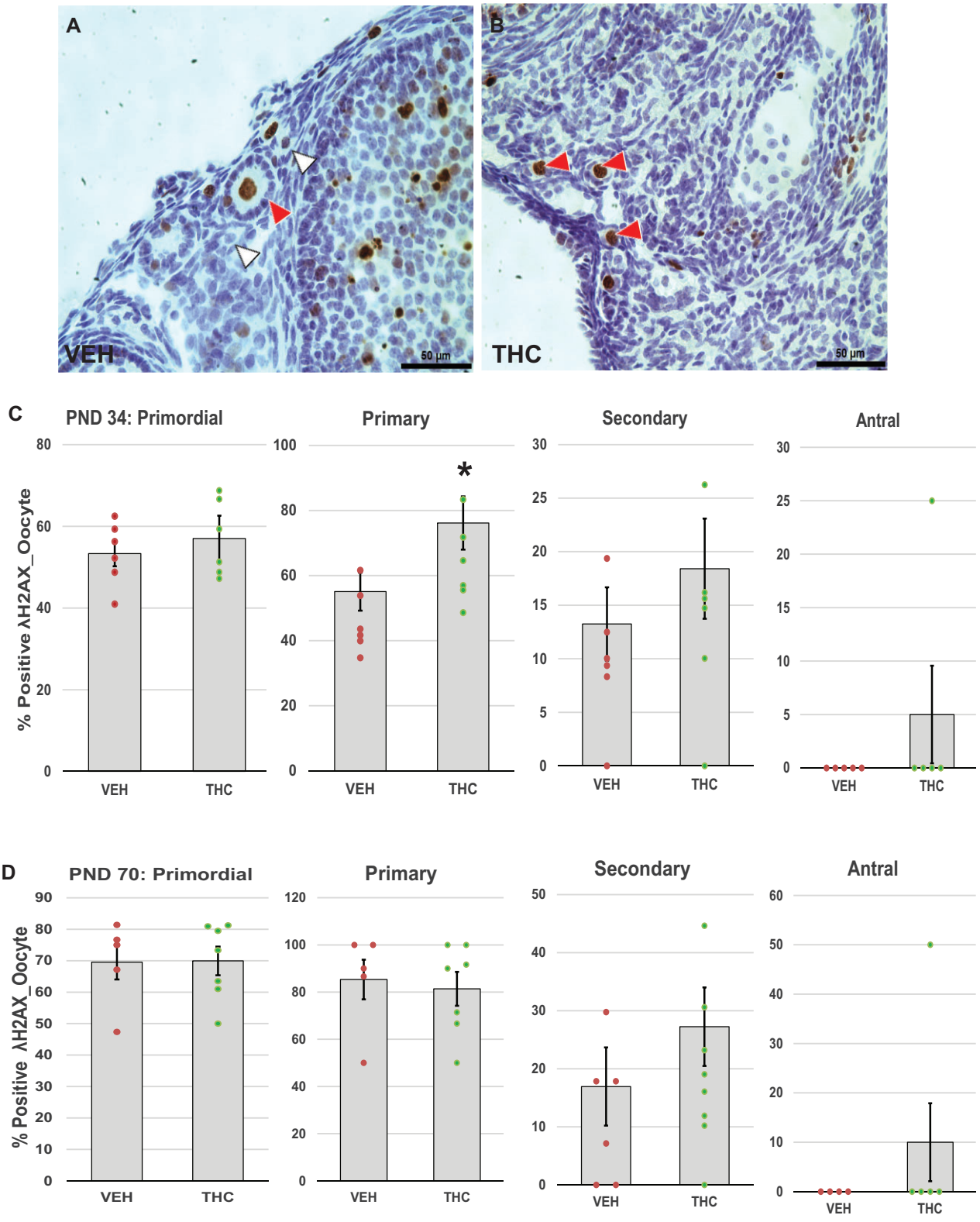

Figure 4. Adolescent THC exposure increases DNA damage in ovarian follicles: Female mice were exposed to THC or vehicle as described for Figure 2 and ovaries were processed for immunostaining for γH2AX as described in Materials and Methods. A and B, Representative images show γH2AX-positive primordial and primary follicles with brown stained nuclei in oocytes in THC (red arrowhead) or vehicle-exposed ovary. White arrowheads indicate γH2AX-negative oocytes in vehicle control ovary. The graphs show the means ± SEM percentages of follicles with γH2AX-positive oocytes in PND 34 (C) and PND 70 (D) ovaries; dots show values for individual mice. THC exposure significantly increased the percentages of primary follicles with γH2AX-positive oocytes in PND 34 mice. *$p < .05$, t test THC versus vehicle. $N = 6–8$/group. Scale bars, 50 µm.

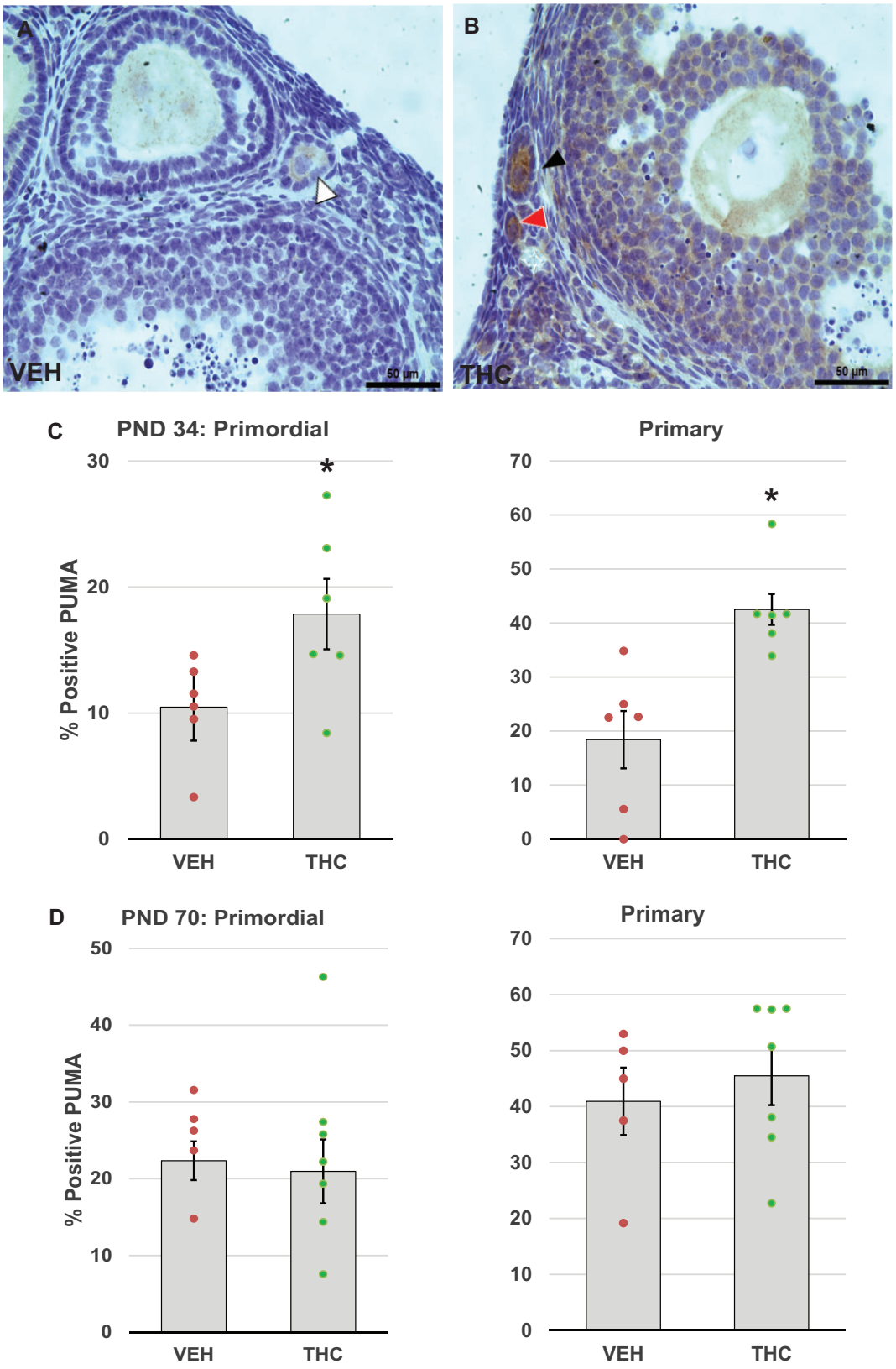

Figure 5. Adolescent THC exposure increases pro-apoptotic PUMA expression in ovarian follicles. Female mice were exposed to THC or vehicle as described for Figure 2, and PND 34 and 70 ovaries were processed immunostaining for p53-upregulated modulator of apoptosis (PUMA) as detailed in Materials and Methods. Representative images of vehicle- (A) and THC-exposed (B) ovaries show PUMA-positive primordial (red arrowhead) and primary (black arrowhead) follicles with brown stained oocytes, as well as a PUMA-negative primary follicle (white arrowhead). C, The graphs show the means ± SEM percentage of PUMA positive primordial and primary follicles in PND34 ovaries. D, The graphs show the means ± SEM percentage of PUMA positive primordial and primary follicles in PND70 ovaries. Dots show values for individual mice. THC exposure significantly increased the percentage of primordial and primary follicles with PUMA-positive oocytes in PND 34 THC mice. *$p < .05$, t test THC versus vehicle. $N = 6–8$/group. Scale bars, 50 µm.

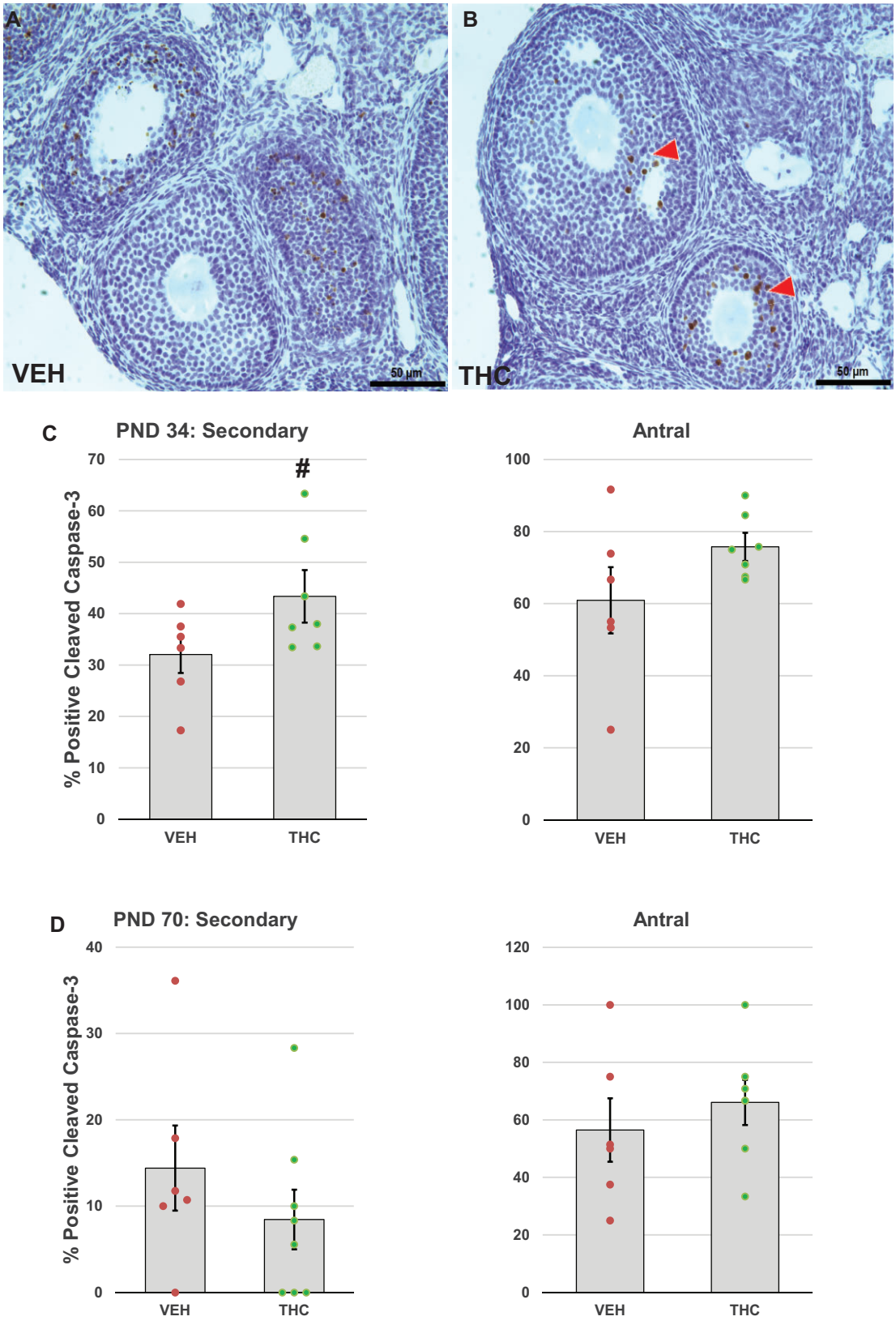

Figure 6. Effects of adolescent THC exposure on caspase-3 activation in ovarian follicles. Female mice were exposed to THC or vehicle as described for Figure 2 and ovaries were processed for immunostaining for activated caspase 3 as detailed in Materials and Methods. Representative images of vehicle- (A) and THC-exposed (B) ovaries show activated caspase 3-positive secondary and antral follicles with brown stained nuclei in granulosa cells (red arrowhead) in the THC-treated ovary. The graphs show the means ± SEM percentage of activated caspase 3-positive secondary and antral follicles on PND 34 (C), 24 h after the last of 4 daily doses, and PND 70 (D), 4 weeks after the last of 14 daily doses; dots show values for individual mice. THC exposure nonsignificantly increased the percentage of secondary follicles with activated caspase 3-positive granulosa cells in PND 34 mice. $^{\#}p = .098$, *t* test THC versus vehicle. $N = 6–8$/group. Scale bars, 50 µm.

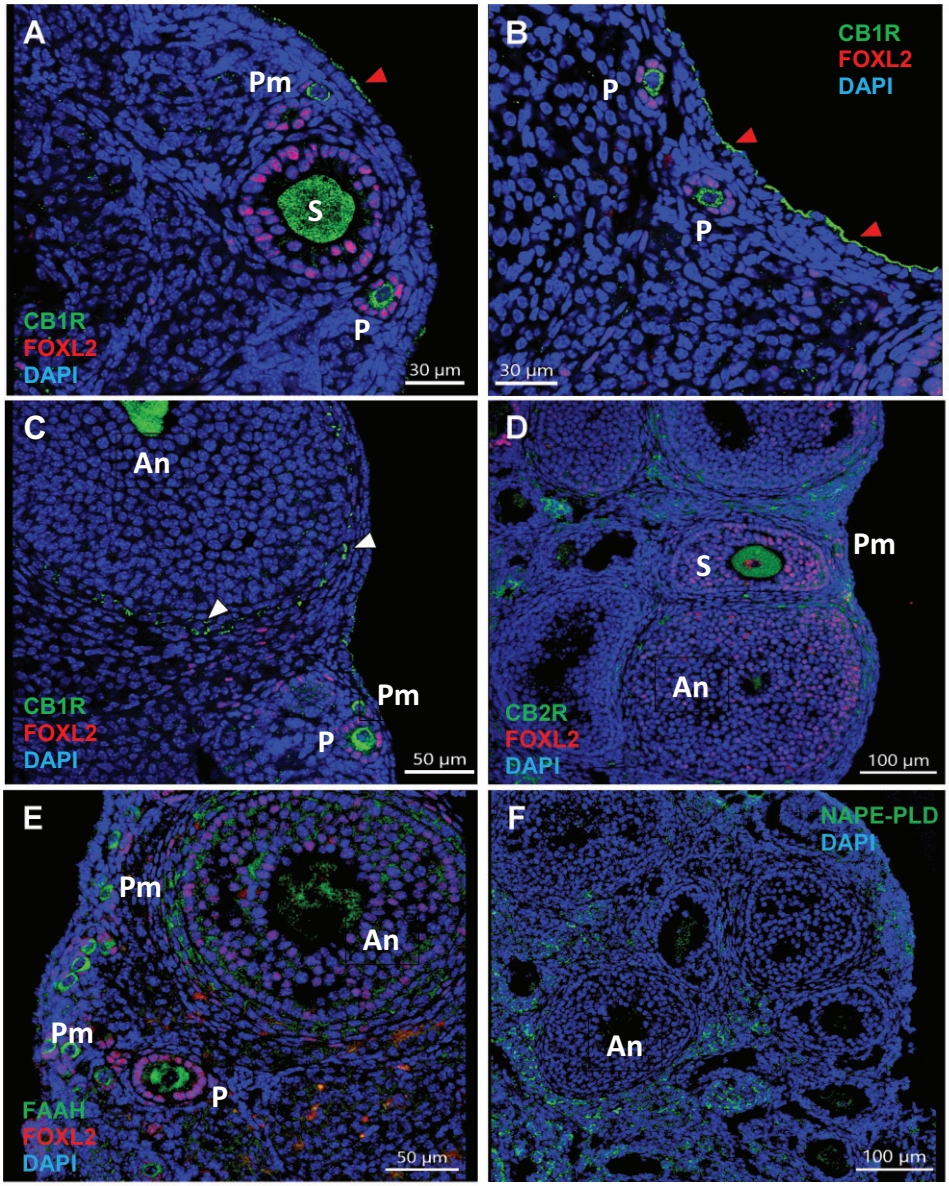

Figure 7. Key components of the ECS are expressed in the mouse ovary. One-month-old female mice were exposed to vehicle as described in Figure 1 and processed for immunolocalization for the cannabinoid CB receptors and AEA-metabolizing enzymes as detailed in Materials and Methods. Images are counterstained with granulosa cell marker FOXL2 (magenta, A–E) and nuclear counterstain DAPI (blue, all images). A–C, Immunofluorescence for cannabinoid receptor 1 (CB1R, green). Images show that CB1R is localized to oocytes of all follicle stages, theca cells of antral follicles (white arrowheads), and ovarian surface epithelium (red arrowheads). D, Immunofluorescence for cannabinoid receptor 2 (CB2R, green). The image shows that CB2R is localized to oocytes of follicles of all stages, theca cells of antral follicles, and interstitial cells. E, Immunofluorescence for fatty acid amide hydrolase (FAAH, green) shows that FAAH is localized to oocytes of all follicle stages and granulosa cells of antral follicles. F, Immunofluorescence for *N*-acylphosphatidylethanolamine-phospholipase D (NAPE-PLD, green) shows localization to theca cells of antral follicles and interstitial cells. An, antral follicle; P, primary follicle; Pm, primordial follicle; S, secondary follicle.

Discussion

The present results indicate that daily adolescent exposure to a low dose of THC, cannabis' intoxicating constituent, disrupts ovarian folliculogenesis in female mice. Strikingly, we found that THC *halved* the finite ovarian reserve of primordial follicles through a mechanism that likely involved induction of DNA damage and pro-apoptotic signaling in primordial and primary follicles as well as accelerated recruitment of primordial follicles into the growing pool. The demonstration that the mouse ovary contains all critical components of the ECS—including CB1R, CB2R, and the AEA-metabolizing enzymes NAPE-PLD and FAAH—points to this signaling complex as a potential molecular substrate for THC's detrimental impact on ovarian structure and function. A key finding was that CB1R and CB2R are strongly expressed in the oocytes of ovarian follicles at various stages of development, particularly in the oocytes of primordial and primary follicles. These immature follicles, which do not respond to gonadotropins, may be responsive to locally generated AEA or 2-AG and might thus be affected by THC exposure.

We selected a dose of THC (5 mg/kg) which produces, in adolescent male mice, human-relevant plasma concentrations of the drug (C_{max} values of 200–400 ng/ml) and only limited pharmacological responses (a modest reduction in core body temperature and no change in motor activity and feeding behavior) (Lee *et al.*, 2022; Torrens *et al.*, 2020). We chose to administer the drug once

Table 2. Localization and signal intensity of ECS components in the mouse ovary by immunofluorescence staining

Follicle Stage	ECS Component	Oocyte	GC	TC
Primordial	CB1R	++	−	×
	CB2R	++	−	×
	FAAH	++	−	×
	NAPE-PLD	−	−	×
Primary	CB1R	++	−	×
	CB2R	++	−	×
	FAAH	++	−	×
	NAPE-PLD	−	−	×
Secondary	CB1R	++	−	+
	CB2R	++	−	+
	FAAH	+	+	+
	NAPE-PLD	−	−	+
Antral, early	CB1R	++	−	++
	CB2R	+	−	+
	FAAH	+	++	+
	NAPE-PLD	−	−	+
Antral, late	CB1R	++	+	++
	CB2R	+	−	+
	FAAH	+	++	+
	NAPE-PLD	−	−	++
Luteal cells	CB1R		+	
	CB2R		+/−	
	FAAH		++	
	NAPE-PLD		−	
Interstitial cells	CB1R		−	
	CB2R		++	
	FAAH		−	
	NAPE-PLD		++	
Surface epithelium	CB1R		++	
	CB2R		−	
	FAAH		−	
	NAPE-PLD		−	

Notes: (−) absent; (+) present; (++) strongly expressed; (+/−) occasionally expressed; and (×) cells not present.

daily, to model frequent low-intensity use by teenagers, and with both acute (4-day exposure) and sub-chronic (14 day exposure) regimens, to capture two possible use patterns in adolescent humans. In mice, an early-mid adolescence has been defined from PND 21 to PND 46 (Adriani *et al.*, 2002; Laviola *et al.*, 2003), which represent teenage humans in our study. The acute study was particularly carried out to evaluate whether THC-mediated apoptosis during early folliculogenesis is a key driver of depletion of the ovarian reserve in adulthood. Despite its relative mildness, our sub-chronic regimen caused an approximately 50% depletion of primordial follicles measured at young adulthood (PND 70). The numbers of healthy antral follicles and corpora lutea were also decreased by the treatment, while the numbers of primary and secondary follicles were not affected. To our knowledge, no other studies have investigated effects of postnatal THC exposure on the ovarian reserve. One study reported that exposure of pregnant rats daily from gestational day 5 to 20 with the same dose of THC as in the present study had no effect on the ovarian reserve (defined as primordial plus primary follicles) of female offspring at PND 90, while prenatal exposure to the CB1/CB2 receptor agonist WIN55212 decreased the ovarian reserve at PND 90 by 40% (Castel *et al.*, 2020).

Depletion of primordial follicles can be caused by follicle death, accelerated activation of quiescent primordial follicles into the growing pool, or both (Kalich-Philosoph *et al.*, 2013; Roness *et al.*, 2013; Spears *et al.*, 2019). We asked therefore whether acute (PND 34, 1 day after the last of 4 daily doses) or sub-chronic (PND 70, 4 weeks after the last of 14 daily doses) THC administration might impact follicle apoptosis and activation. Ki67 immunostaining was used as a specific marker of mitosis to measure follicle activation based on granulosa cell proliferation (Scholzen and Gerdes, 2000). Our classification rubric grouped follicles transitioning from the primordial to the primary stage with primary follicles. Therefore, the increased percentage of Ki67-positive primary follicles in THC-treated mice provides evidence for accelerated recruitment of primordial follicles into the growing pool. Further support for this mechanism of primordial follicle depletion comes from our observation of significantly decreased antral follicle numbers in the THC-treated mice. Antral and secondary follicles produce anti-Müllerian hormone (AMH), which acts in a paracrine manner to inhibit activation of primordial follicles (Durlinger *et al.*, 1999; Visser and Themmen, 2005). With decreased numbers of antral follicles, less AMH is produced, resulting in increased activation of primordial follicles.

We also investigated the effects of THC exposure on apoptotic death of ovarian follicles. DNA damage is a well-known inducer of apoptosis; therefore, we assessed follicle DNA damage using γH2AX immunostaining. We observed that acute adolescent exposure to THC increased γH2AX immunoreactivity in the oocytes of primary follicles in PND 34. We and others previously reported that the pro-apoptotic BCL2 family protein PUMA is a key initiator of oocyte apoptosis in primordial and primary follicles in mice following DNA-damaging gamma-irradiation (Kerr *et al.*, 2012), iron ion-irradiation (Mishra *et al.*, 2016), and administration of the antineoplastic agent cyclophosphamide (Nguyen *et al.*, 2018). In the present study, immunoreactivity for PUMA was increased in oocytes of primordial and primary follicles on PND 34, 24 h after the fourth dose of THC. We did not observe increases in the numbers of primordial and primary follicles with activated caspase 3-positive oocytes, despite the increases in γH2AX and PUMA immunostaining in these follicles. It is possible that we did not observe activated caspase 3 in these follicles because we examined the ovaries too late after the DNA damage-inducing stimulus. Others have shown that TdT-mediated dUTP nick end labeling (TUNEL), a late marker of apoptosis peaks in primordial follicles at 8 h after exposure to cisplatin or cyclophosphamide, while γH2AX immunoreactivity persists for at least 24 h (Nguyen *et al.*, 2019). Our results are consistent with previous studies which reported that THC can cause apoptosis in C6 glioma cells (Sánchez *et al.*, 1998), primary cultures of rat hippocampal neurons via DNA damage (Chan *et al.*, 1998), and rat spermatozoa (Nahas *et al.*, 2002).

Cannabinoid signaling is mediated by G-protein-coupled CB1R and CB2R (Howlett, 2002; Ligresti *et al.*, 2016). CB1R is highly expressed in the CNS but also present in peripheral tissues. CB2R is mainly found in immune cells, though low levels of expression are also found in other cell lineages (Demuth and Molleman, 2006). Although the presence of CBRs in human and rat ovaries has been previously reported, the ovarian localization of these proteins in the mouse has not previously been described. In human ovaries, immunohistochemical experiments demonstrated that CB1R and CB2R are present in oocytes and granulosa cells of primordial, primary, secondary, and antral follicles and in corpora lutea (El-Talatini *et al.*, 2009). Both receptors were also detected in the theca cells of growing follicles in human ovaries (El-Talatini *et al.*, 2009). In rat ovaries, immunofluorescence detection revealed that CB1R was expressed in the OSE, granulosa cells of antral follicles, and the luteal cells of corpus luteum; however, granulosa cells of secondary follicles, oocytes, and theca cells were not found to express CB1R (Bagavandoss and Grimshaw, 2010). CB2R was detected exclusively in oocytes of

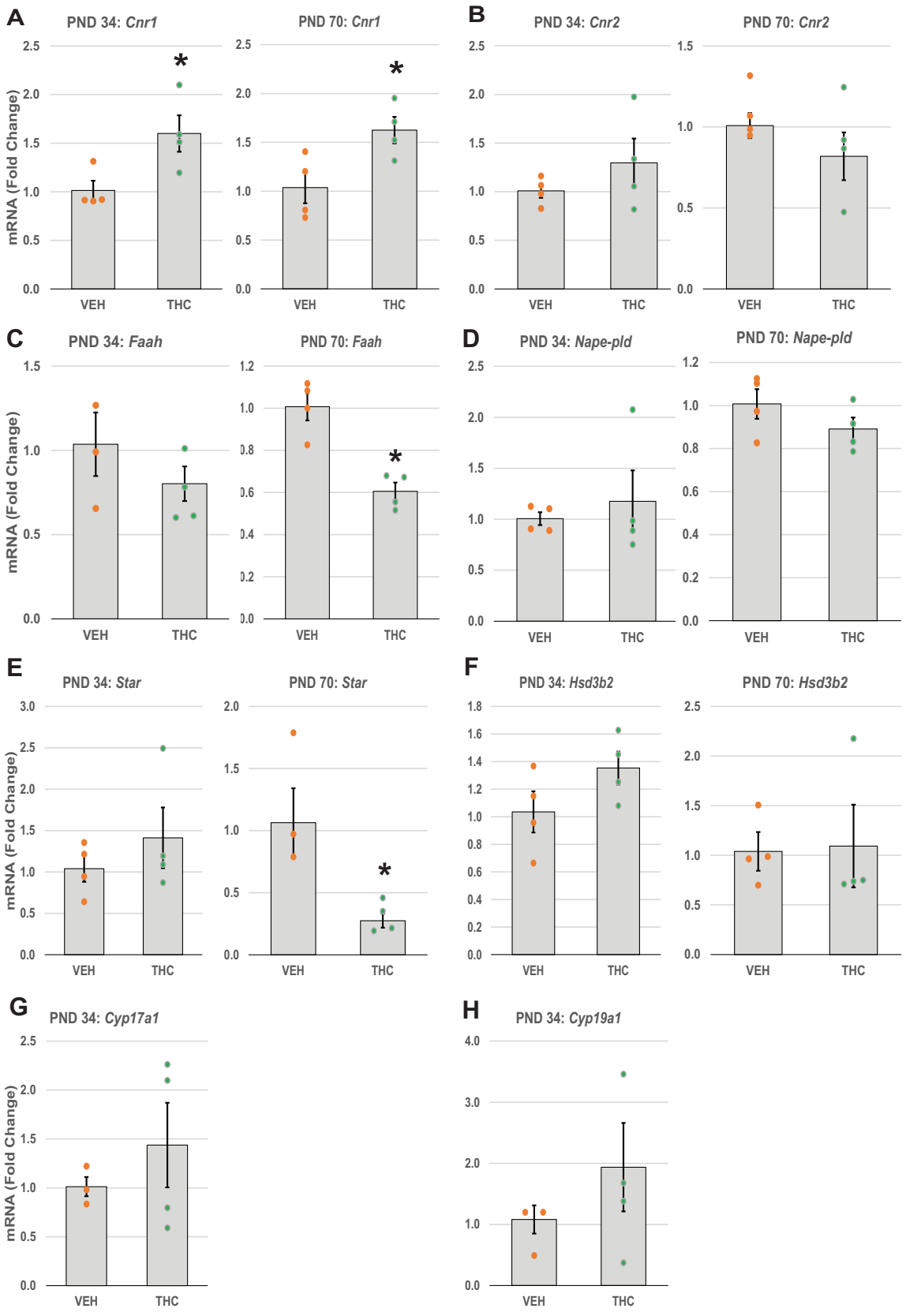

Figure 8. Effects of adolescent THC exposure on quantitative mRNA expression of ECS and steroidogenesis genes. Female mice were exposed to THC or vehicle as described for Figure 2. The freshly harvested ovaries were processed for RNA extraction and qRT-PCR as detailed in Materials and Methods. The graph bars show the means ± SEM mRNA levels; dots show values for individual mice. The relative expression of mRNA transcripts related to (A and B) cannabinoid CB receptors (*Cnr1*, *Cnr2*), (C and D) AEA-metabolizing enzymes (*Faah* and *Nape-pld*), and (E) steroidogenic protein (*Star*) and (F–H) enzymes (*Hsd3b2*, *Cyp17a1*, and *Cyp19a1*) are shown for the experimental groups: THC and vehicle. The experiments were performed in triplicate using PND 34 and PND 70 ovaries ($N = 3$–4/group). *$p < .05$, *t* test THC versus vehicle.

both secondary and antral follicles, but not in granulosa cells of the follicles in rat ovaries (Bagavandoss and Grimshaw, 2010). In the present study, we confirmed that both CB1R and CB2R are present in mouse ovaries and mainly localized to the oocytes of primordial, primary, secondary, and antral follicles and to theca cells of the growing antral follicles. In contrast to the results reported for humans and rats, we did not detect CB1R in granulosa cells at any stages of follicular development. As seen in the rat, in the present study, CB1R was also distinctly localized to the OSE in mouse ovaries. Corpora lutea also expressed CB1R, but with a patchy distribution. CB2R was expressed in the oocytes of all follicle types in a similar manner as CB1R, in the theca cells of antral follicles, and in ovarian interstitial/stromal cells. The differences in subcellular localization of CB1R and CB2R in our study compared to prior studies may be due to species-specific and/or age-specific differences. Our immunofluorescence imaging results revealed that strong expression of CB1R and CB2R in the oocytes at all follicular development stages and in hormone-producing theca cells of antral follicles in the ovary points to the involvement of local CBRs-mediated signaling in regulating ovarian steroidogenesis and folliculogenesis. We also observed that THC-treated adolescent female mice exhibited a persistently elevated expression of ovarian *Cnr1* mRNA. These observations, together with our finding of increased primordial follicle activation in THC-exposed ovaries, raise the possibility that the persistent activation of CB1R in oocytes may trigger signaling pathways regulating follicle activation, such as KIT, PI3K/AKT, neurotrophins, and platelet-derived growth factor (Nilsson *et al.*, 2006; Ojeda *et al.*, 2000; Reddy *et al.*, 2010).

AEA levels are tightly controlled by NAPE-PLD and FAAH (Piomelli and Mabou Tagne, 2022). FAAH, the enzyme responsible for the degradation of AEA, was reportedly expressed only in theca cells of secondary and antral follicles, the corpus luteum and corpus albicans, whereas NAPE-PLD, the enzyme responsible for the formation of AEA, was detected in the granulosa and theca cells of growing secondary and antral follicles, corpora lutea, and albicans in human ovaries (El-Talatini *et al.*, 2009). In oocytes, NAPE-PLD was sporadically detectable only in primordial follicles, while FAAH was not detected in oocytes of any follicle types (El-Talatini *et al.*, 2009). By contrast, we observed that FAAH is expressed in the oocytes of primordial, primary, secondary, and antral follicles in mice. Interestingly, FAAH is also strongly expressed in the granulosa cells of antral follicles. NAPE-PLD localized to the theca cells of antral follicles and interstitial cells; however, NAPE-PLD immunoreactivity was absent from the oocytes of the ovarian follicles. Expression of *Cn2r and Nape-pld* mRNA was not affected by adolescent THC exposure, whereas expression of *Faah* mRNA at PND 70 was significantly reduced in THC-treated ovaries compared to PND 34 ovaries. This difference in *Faah* mRNA expression may be due to the observed decline in the number of healthy antral follicles in which FAAH is strongly expressed in granulosa cells. THC-mediated destruction of ovarian follicles could be exerted through central or local CB1R, or both. We found that both CB1R and FAAH are expressed in hormone-releasing cells of antral follicles in the ovary and *Cn1r* mRNA levels are persistently up-regulated, whereas *Faah* mRNA levels are down-regulated in THC-treated mice. THC-mediated down-regulation of *Faah* mRNA would be predicted to result in elevated levels of AEA which would increase activation of CB1R in the ovary.

Significant loss of ovarian antral follicles can lead to impaired steroidogenesis due to concurrent loss of steroidogenic cells in the growing follicles. We observed that mice treated with THC during adolescence had significantly fewer mature antral follicles when they reached adulthood. In line with this, adolescent THC exposure significantly decreased *Star* mRNA expression, while mRNA expression of steroidogenic enzymes (*Hsd3b2*, *Cyp17a1*, and *Cyp19a1*) was not affected by THC treatment, which indicates that StAR could be a target protein of THC exposure. We observed that StAR protein is expressed in the oocytes of primary, secondary, and antral follicles and in the theca cells of preovulatory follicles. Strong StAR expression has previously been reported in theca cells of human and sheep ovaries (Kiriakidou *et al.*, 1996; Logan *et al.*, 2002). Similar to our observation, *Star* mRNA expression was also reported in oocytes of follicles at all stages of development in adult sheep ovaries (Logan *et al.*, 2002). LH-induced cAMP signaling results in estradiol production in follicular steroidogenic cells by rapidly increasing *Star* mRNA levels (Caron *et al.*, 1997; Clark *et al.*, 1995; Sandhoff *et al.*, 1998; Sugawara *et al.*, 1997). In human tissues, treatment with cAMP analog increases expression of *Star* mRNA in theca interna cells of human preovulatory follicles (Kiriakidou *et al.*, 1996). LH binding to its receptor activates adenylate cyclase, whereas THC inhibits adenylyl cyclase (Bayewitch *et al.*, 1995; Howlett and Fleming, 1984; Vogel *et al.*, 1993) through the activation of CBRs (Bayewitch *et al.*, 1995; Slipetz *et al.*, 1995). Therefore, it is possible that THC downregulates the transcription of *Star* mRNA by regulating LH or cAMP levels, or both. However, it will require a dedicated set of studies to explore the possibility that THC-mediated dysregulation of cAMP-dependent *Star* mRNA expression could disrupt the steroid biosynthetic machinery in the ovary.

In conclusion, we have shown that daily exposure of female adolescent mice to relatively low doses of THC causes a significant decrease of the ovarian reserve, which persists until adulthood and is likely due to a persistent acceleration of follicle recruitment into the growing pool and apoptotic death of primordial and primary follicles. Given the cannabis use in adolescence is increasing, at least in part due to the increased accessibility of cannabis products in North America in the past two decades (Hammond *et al.*, 2022), it is imperative to elucidate the consequences of early-life exposure to cannabis on reproductive health in adulthood. Our findings provide unexpected new insights into the long-term impact of THC on reproductive function and aging, which may be relevant to women who made frequent use of cannabis during their teenage years.

Supplementary data

Supplementary data are available at *Toxicological Sciences* online.

Declaration of conflicting interests

The author/authors declared no potential conflicts of interest with respect to the research, authorship, and/or publication of this article.

Authors' roles

J.L., D.P., and U.L. conceived and designed the study. S.V.M. treated and provided mice. J.L., H.-L.L., J.N., J.S., S.G., C.Q., and E.S. contributed to data collection. K.M. provided reagents. J.L., K.-M.J., and U.L. analyzed and interpreted the data. J.L., K.-M.J., D.P., and U.L. contributed to writing the article. All the authors reviewed and approved the final version of the article.

Funding

National Institutes of Health (NIH) National Institute on Drug Abuse (NIDA) Center, Impact of Cannabinoids across the Lifespan (grant P50DA044118), Pilot Grants to U.L. and J.L.; NIH (R01ES020454) to U.L. The authors wish to acknowledge the support of the UC Irvine Optical Biology Shared Resource, supported by the National Cancer Institute (NCI) NIH Chao Family Comprehensive Cancer Center (award number P30CA062203) and the UC Irvine Center for Complex Biological Systems Support Grant (award number P50GM076516). UC Irvine Summer Undergraduate Research Program fellowships to J.N. and C.Q.

Acknowledgments

The authors thank Jana Chen for help with tissue collections and sample preparations and Victoria Inshishian for performing the THC injections.

Data availability

The data underlying this article are available in the article and/or will be shared on reasonable request to the corresponding author.

References

Adriani, W., Macrì, S., Pacifici, R., and Laviola, G. (2002). Peculiar vulnerability to nicotine oral self-administration in mice during early adolescence. *Neuropsychopharmacology* **27**, 212–224.

Almirez, R. G., Smith, C. G., and Asch, R. H. (1983). The effects of marijuana extract and delta 9-tetrahydrocannabinol on luteal function in the rhesus monkey. *Fertil Steril* **39**, 212–217.

Asch, R., Simerly, C., Ord, T., Ord, V. A., and Schatten, G. (1995). The stages at which human fertilization arrests: microtubule and chromosome configurations in inseminated oocytes which failed to complete fertilization and development in humans. *Hum. Reprod.* **10**, 1897–1906.

Asch, R. H., Smith, C. G., Siler-Khodr, T. M., and Pauerstein, C. J. (1981). Effects of delta 9-tetrahydrocannabinol during the follicular phase of the rhesus monkey (*Macaca mulatta*). *J. Clin. Endocrinol. Metab.* **52**, 50–55.

Bagavandoss, P., and Grimshaw, S. (2010). Temporal and spatial distribution of the cannabinoid receptors (CB1, CB2) and fatty acid amide hydroxylase in the rat ovary. *Anat. Rec. (Hoboken)* **293**, 1425–1432.

Bayewitch, M., Avidor-Reiss, T., Levy, R., Barg, J., Mechoulam, R., and Vogel, Z. (1995). The peripheral cannabinoid receptor: adenylate cyclase inhibition and G protein coupling. *FEBS Lett.* **375**, 143–147.

Brents, L. K. (2016). Marijuana, the endocannabinoid system and the female reproductive system. *Yale J. Biol. Med.* **89**, 175–191.

Caron, K. M., Ikeda, Y., Soo, S. C., Stocco, D. M., Parker, K. L., and Clark, B. J. (1997). Characterization of the promoter region of the mouse gene encoding the steroidogenic acute regulatory protein. *Mol. Endocrinol.* **11**, 138–147.

Castel, P., Barbier, M., Poumerol, E., Mandon-Pépin, B., Tassistro, V., Lepidi, H., Pelissier-Alicot, A. L., Manzoni, O. J., and Courbiere, B. (2020). Prenatal cannabinoid exposure alters the ovarian reserve in adult offspring of rats. *Arch. Toxicol.* **94**, 4131–4141.

Chan, G. C., Hinds, T. R., Impey, S., and Storm, D. R. (1998). Hippocampal neurotoxicity of delta9-tetrahydrocannabinol. *J. Neurosci.* **18**, 5322–5332.

Clark, B. J., Soo, S. C., Caron, K. M., Ikeda, Y., Parker, K. L., and Stocco, D. M. (1995). Hormonal and developmental regulation of the steroidogenic acute regulatory protein. *Mol. Endocrinol.* **9**, 1346–1355.

Demuth, D. G., and Molleman, A. (2006). Cannabinoid signalling. *Life Sci.* **78**, 549–563.

Desmeules, P., and Devine, P. J. (2006). Characterizing the ovotoxicity of cyclophosphamide metabolites on cultured mouse ovaries. *Toxicol. Sci.* **90**, 500–509.

Devane, W. A., Dysarz, F. A., 3rd, Johnson, M. R., Melvin, L. S., and Howlett, A. C. (1988). Determination and characterization of a cannabinoid receptor in rat brain. *Mol. Pharmacol.* **34**, 605–613.

Devane, W. A., Hanus, L., Breuer, A., Pertwee, R. G., Stevenson, L. A., Griffin, G., Gibson, D., Mandelbaum, A., Etinger, A., and Mechoulam, R. (1992). Isolation and structure of a brain constituent that binds to the cannabinoid receptor. *Science* **258**, 1946–1949.

Di Marzo, V., Fontana, A., Cadas, H., Schinelli, S., Cimino, G., Schwartz, J. C., and Piomelli, D. (1994). Formation and inactivation of endogenous cannabinoid anandamide in central neurons. *Nature* **372**, 686–691.

Durlinger, A. L. L., Kramer, P., Karels, B., de Jong, F. H., Uilenbroek, J. T. J., Grootegoed, J. A., and Themmen, A. P. N. (1999). Control of primordial follicle recruitment by anti-Müllerian hormone in the mouse ovary. *Endocrinology* **140**, 5789–5796.

El-Talatini, M. R., Taylor, A. H., Elson, J. C., Brown, L., Davidson, A. C., and Konje, J. C. (2009). Localisation and function of the endocannabinoid system in the human ovary. *PLoS One*. **4**, e4579.

Fenwick, M. A., and Hurst, P. R. (2002). Immunohistochemical localization of active caspase-3 in the mouse ovary: growth and atresia of small follicles. *Reproduction* **124**, 659–665.

Fezza, F., Bari, M., Florio, R., Talamonti, E., Feole, M., and Maccarrone, M. (2014). Endocannabinoids, related compounds and their metabolic routes. *Molecules* **19**, 17078–17106.

Freund, T. F., Katona, I., and Piomelli, D. (2003). Role of endogenous cannabinoids in synaptic signaling. *Physiol. Rev.* **83**, 1017–1066.

Gaoni, Y., and Mechoulam, R. (1964). Isolation, structure and partial synthesis of an active constituent of hashish. *J. Am. Chem. Soc.* **86**, 1646–1647.

Gore-Langton, R. E., and Armstrong, D. T. (1994). Follicular steroidogenesis and its control. In *The Physiology of Reproduction* (E. Knobil and J. D. Neill, Eds.), 2nd ed, pp. 571–627. Raven Press, New York, NY.

Greene, A. D., Patounakis, G., and Segars, J. H. (2014). Genetic associations with diminished ovarian reserve: a systematic review of the literature. *J. Assist. Reprod. Genet.* **31**, 935–946.

Hammond, D., Goodman, S., Wadsworth, E., Freeman, T. P., Kilmer, B., Schauer, G., Pacula, R. L., and Hall, W. (2022). Trends in the use of cannabis products in Canada and the USA, 2018–2020: findings from the international cannabis policy study. *Int. J. Drug Policy* **105**, 103716.

Hannon, P. R., Brannick, K. E., Wang, W., Gupta, R. K., and Flaws, J. A. (2015). Di(2-ethylhexyl) phthalate inhibits antral follicle growth, induces atresia, and inhibits steroid hormone production in cultured antral follicles. *Toxicol. Appl. Pharmacol.* **284**, 42–53.

Hirshfield, A. N. (1988). Size-frequency analysis of atresia in cycling rats. *Biol. Reprod.* **38**, 1181–1188.

Howlett, A. C. (2002). The cannabinoid receptors. *Prostaglandins Other Lipid Mediat.* **68–69**, 619–631.

Howlett, A. C., and Fleming, R. M. (1984). Cannabinoid inhibition of adenylate cyclase. Pharmacology of the response in neuroblastoma cell membranes. *Mol. Pharmacol.* **26**, 532–538.

Huestis, M. A. (2007). Human cannabinoid pharmacokinetics. *Chem. Biodivers.* **4**, 1770–1804.

Huestis, M. A., and Cone, E. J. (2004). Relationship of delta 9-tetrahydrocannabinol concentrations in oral fluid and plasma after controlled administration of smoked cannabis. *J. Anal. Toxicol.* **28**, 394–399.

Iversen, L. (2003). Cannabis and the brain. *Brain* **126**, 1252–1270.

Jefcoate, C. R., McNamara, B. C., Artemenko, I., and Yamazaki, T. (1992). Regulation of cholesterol movement to mitochondrial cytochrome p450scc in steroid hormone synthesis. *J. Steroid Biochem. Mol. Biol.* **43**, 751–767.

Juengel, J. L., and McNatty, K. P. (2005). The role of proteins of the transforming growth factor-β superfamily in the intraovarian regulation of follicular development. *Hum. Reprod. Update* **11**, 144–161.

Jung, K. M., and Piomelli, D. (2022). Cannabinoids and endocannabinoids. In *Neuroscience in the 21st Century* (D. Pfaff and N. Volkow, Eds.), p. 1–29. Springer, New York, NY. Available at: https://link.springer.com/referenceworkentry/10.1007/978-1-4614-6434-1_136-2#DOI

Kalich-Philosoph, L., Roness, H., Carmely, A., Fishel-Bartel, M., Ligumsky, H., Paglin, S., Wolf, I., Kanety, H., Sredni, B., and Meirow, D. (2013). Cyclophosphamide triggers follicle activation and "burnout"; as101 prevents follicle loss and preserves fertility. *Sci Transl Med* **5**, 185ra162.

Kano, M., Ohno-Shosaku, T., Hashimotodani, Y., Uchigashima, M., and Watanabe, M. (2009). Endocannabinoid-mediated control of synaptic transmission. *Physiol. Rev.* **89**, 309–380.

Kerr, J. B., Hutt, K. J., Michalak, E. M., Cook, M., Vandenberg, C. J., Liew, S. H., Bouillet, P., Mills, A., Scott, C. L., Findlay, J. K., *et al.* (2012). DNA damage-induced primordial follicle oocyte apoptosis and loss of fertility require tap63-mediated induction of *Puma* and *Noxa*. *Mol. Cell* **48**, 343–352.

Kinner, A., Wu, W., Staudt, C., and Iliakis, G. (2008). Γ-h2ax in recognition and signaling of DNA double-strand breaks in the context of chromatin. *Nucleic Acids Res.* **36**, 5678–5694.

Kiriakidou, M., McAllister, J. M., Sugawara, T., and Strauss, J. F. 3rd. (1996). Expression of steroidogenic acute regulatory protein (star) in the human ovary. *J. Clin. Endocrinol. Metab.* **81**, 4122–4128.

Laviola, G., Macrì, S., Morley-Fletcher, S., and Adriani, W. (2003). Risk-taking behavior in adolescent mice: psychobiological determinants and early epigenetic influence. *Neurosci. Biobehav. Rev.* **27**, 19–31.

LaVoie, H. A. (2017). Transcriptional control of genes mediating ovarian follicular growth, differentiation, and steroidogenesis in pigs. *Mol. Reprod. Dev.* **84**, 788–801.

Lee, H.-L., Jung, K.-M., Fotio, Y., Squire, E., Palese, F., Lin, L., Torrens, A., Ahmed, F., Mabou Tagne, A., Ramirez, J., *et al.* (2022). Frequent low-dose δ9-tetrahydrocannabinol in adolescence disrupts microglia homeostasis and disables responses to microbial infection and social stress in young adulthood. *Biol. Psychiatry.* **92**, 845–860.

Lee, S. G., Kim, J. Y., Chung, J. Y., Kim, Y. J., Park, J. E., Oh, S., Yoon, Y. D., Yoo, K. S., Yoo, Y. H., and Kim, J. M. (2013). Bisphenol a exposure during adulthood causes augmentation of follicular atresia and luteal regression by decreasing 17β-estradiol synthesis via downregulation of aromatase in rat ovary. *Environ, Health Perspect*, **121**, 663–669.

Lei, L., and Spradling, A. C. (2013). Female mice lack adult germ-line stem cells but sustain oogenesis using stable primordial follicles. *Proc. Natl. Acad. Sci. U. S. A.* **110**, 8585–8590.

Ligresti, A., De Petrocellis, L., and Di Marzo, V. (2016). From phytocannabinoids to cannabinoid receptors and endocannabinoids: pleiotropic physiological and pathological roles through complex pharmacology. *Physiol. Rev.* **96**, 1593–1659.

Lim, J., Lawson, G. W., Nakamura, B. N., Ortiz, L., Hur, J. A., Kavanagh, T. J., and Luderer, U. (2013). Glutathione-deficient mice have increased sensitivity to transplacental benzo[a]pyrene-induced premature ovarian failure and ovarian tumorigenesis. *Cancer Res.* **73**, 908–917.

Lim, J., Ramesh, A., Shioda, T., Leon Parada, K., and Luderer, U. (2022). Sex differences in embryonic gondal transcriptomes and benzop[a]pyrene metabolite levels after transplacental exposure. *Endocrinology* **163**, 1–17.

Livak, K. J., and Schmittgen, T. D. (2001). Analysis of relative gene expression data using real-time quantitative pcr and the $2^{-\delta\delta}$ct method. *Methods* **25**, 402–408.

Logan, K. A., Juengel, J. L., and McNatty, K. P. (2002). Onset of steroidogenic enzyme gene expression during ovarian follicular development in sheep. *Biol. Reprod.* **66**, 906–916.

Lu, H. C., and Mackie, K. (2021). Review of the endocannabinoid system. *Biol Psychiatry Cogn. Neurosci. Neuroimaging* **6**, 607–615.

Luderer, U. (2014). Ovarian toxicity from reactive oxygen species. In *Endocrine Disrupters* (G. Litwack, Ed.), pp. 99–127. Academic Press/Elsevier, Burlington, VT.

Mackie, K. (2005). Distribution of cannabinoid receptors in the central and peripheral nervous system. *Handb. Exp. Pharmacol.* **168**, 299–325.

Matsuda, L. A., Lolait, S. J., Brownstein, M. J., Young, A. C., and Bonner, T. I. (1990). Structure of a cannabinoid receptor and functional expression of the cloned cDNA. *Nature* **346**, 561–564.

Mechoulam, R., Ben-Shabat, S., Hanus, L., Ligumsky, M., Kaminski, N. E., Schatz, A. R., Gopher, A., Almog, S., Martin, B. R., and Compton, D. R. (1995). Identification of an endogenous 2-monoglyceride, present in canine gut, that binds to cannabinoid receptors. *Biochem. Pharmacol.* **50**, 83–90.

Mendelson, J. H., Mello, N. K., Ellingboe, J., Skupny, A. S., Lex, B. W., and Griffin, M. (1986). Marihuana smoking suppresses luteinizing hormone in women. *J. Pharmacol. Exp. Ther.* **237**, 862–866.

Miech, R. A., Johnston, L. D., O'Malley, P. M., Bachman, J. G., Schulenberg, J. E., and Patrick, M. E. (2021). *Monitoring the Future: National Survey Results on Drug Use 1975-2021*. National Institute on Drug Abuse, Ann Arbor.

Miller, W. L., and Auchus, R. J. (2011). The molecular biology, biochemistry, and physiology of human steroidogenesis and its disorders. *Endocr. Rev.* **32**, 81–151.

Mishra, B., Ortiz, L., and Luderer, U. (2016). Charged iron particles, typical of space radiation, destroy ovarian follicles. *Hum. Reprod.* **31**, 1816–1826.

Munro, S., Thomas, K. L., and Abu-Shaar, M. (1993). Molecular characterization of a peripheral receptor for cannabinoids. *Nature* **365**, 61–65.

Myers, M., Britt, K. L., Wreford, N. G. M., Ebling, F. J. P., and Kerr, J. B. (2004). Methods for quantifying follicular numbers within the mouse ovary. *Reproduction* **127**, 569–580.

Myers, M., Morgan, F. H., Liew, S. H., Zerafa, N., Gamage, T. U., Sarraj, M., Cook, M., Kapic, I., Sutherland, A., Scott, C. L., *et al.* (2014). Puma regulates germ cell loss and primordial follicle endowment in mice. *Reproduction* **148**, 211–219.

Myers, M. B., McKim, K. L., Meng, F., and Parsons, B. L. (2015). Low-frequency KRAS mutations are prevalent in lung adenocarcinomas. *Per. Med.* **12**, 83–98.

Nahas, G. G., Frick, H. C., Lattimer, J. K., Latour, C., and Harvey, D. (2002). Pharmacokinetics of THC in brain and testis, male gametotoxicity and premature apoptosis of spermatozoa. *Hum. Psychopharmacol.* **17**, 103–113.

Nelson, L. M. (2009). Primary ovarian insufficiency. *N Engl. J. Med.* **360**, 606–614.

Nguyen, Q. N., Zerafa, N., Liew, S. H., Findlay, J. K., Hickey, M., and Hutt, K. J. (2019). Cisplatin- and cyclophosphamide-induced primordial follicle depletion is caused by direct damage to oocytes. *Mol. Hum. Reprod.* **25**, 433–444.

Nguyen, Q. N., Zerafa, N., Liew, S. H., Morgan, F. H., Strasser, A., Scott, C. L., Findlay, J. K., Hickey, M., and Hutt, K. J. (2018). Loss of puma protects the ovarian reserve during DNA-damaging chemotherapy and preserves fertility. *Cell Death Dis.* **9**, 618.

Nilsson, E. E., Detzel, C., and Skinner, M. K. (2006). Platelet-derived growth factor modulates the primordial to primary follicle transition. *Reproduction* **131**, 1007–1015.

Ojeda, S. R., Romero, C., Tapia, V., and Dissen, G. A. (2000). Neurotrophic and cell-cell dependent control of early follicular development. *Mol. Cell. Endocrinol.* **163**, 67–71.

Paria, B. C., Ma, W., Andrenyak, D. M., Schmid, P. C., Schmid, H. H., Moody, D. E., Deng, H., Makriyannis, A., and Dey, S. K. (1998). Effects of cannabinoids on preimplantation mouse embryo development and implantation are mediated by brain-type cannabinoid receptors. *Biol. Reprod.* **58**, 1490–1495.

Piomelli, D. (2003). The molecular logic of endocannabinoid signalling. *Nat. Rev. Neurosci.* **4**, 873–884.

Piomelli, D., Astarita, G., and Rapaka, R. (2007). A neuroscientist's guide to lipidomics. *Nat. Rev. Neurosci.* **8**, 743–754.

Piomelli, D., and Mabou Tagne, A. (2022). Endocannabinoid-based therapies. *Annu. Rev. Pharmacol. Toxicol.* **62**, 483–507.

Rebar, R. W. (2005). Mechanisms of premature menopause. *Endocrinol. Metab. Clin. North Am.* **34**, 923–933, ix.

Reddy, P., Adhikari, D., Zheng, W., Liang, S., Hämäläinen, T., Tohonen, V., Ogawa, W., Noda, T., Volarevic, S., Huhtaniemi, I., *et al.* (2009). Pdk1 signaling in oocytes controls reproductive aging and lifespan by manipulating the survival of primordial follicles. *Hum. Mol. Genet.* **18**, 2813–2824.

Reddy, P., Liu, L., Adhikari, D., Jagarlamudi, K., Rajareddy, S., Shen, Y., Du, C., Tang, W., Hämäläinen, T., Peng, S. L., *et al.* (2008). Oocyte-specific deletion of *Pten* causes premature activation of the primordial follicle pool. *Science* **319**, 611–613.

Reddy, P., Zheng, W., and Liu, K. (2010). Mechanisms maintaining the dormancy and survival of mammalian primordial follicles. *Trends Endocrinol. Metab.* **21**, 96–103.

Riches, L. C., Lynch, A. M., and Gooderham, N. J. (2008). Early events in the mammalian response to DNA double-strand breaks. *Mutagenesis* **23**, 331–339.

Roness, H., Gavish, Z., Cohen, Y., and Meirow, D. (2013). Ovarian follicle burnout: a universal phenomenon? *Cell Cycle* **12**, 3245–3246.

SAMSHA. (2020). *2020 National Survey of Drug Use and Health (NSDUH) Releases*. Substance Abuse and Mental Health Services Administration, Rockville, MD.

Sánchez, C., Galve-Roperh, I., Canova, C., Brachet, P., and Guzmán, M. (1998). Delta9-tetrahydrocannabinol induces apoptosis in c6 glioma cells. *FEBS Lett.* **436**, 6–10.

Sandhoff, T. W., Hales, D. B., Hales, K. H., and McLean, M. P. (1998). Transcriptional regulation of the rat steroidogenic acute regulatory protein gene by steroidogenic factor 1. *Endocrinology* **139**, 4820–4831.

Scholzen, T., and Gerdes, J. (2000). The Ki-67 protein: from the known to the unknown. *J, Cell, Physiol*, **182**, 311–322.

Slipetz, D. M., O'Neill, G. P., Favreau, L., Dufresne, C., Gallant, M., Gareau, Y., Guay, D., Labelle, M., and Metters, K. M. (1995). Activation of the human peripheral cannabinoid receptor results in inhibition of adenylyl cyclase. *Mol. Pharmacol.* **48**, 352–361.

Smith, C. G., Besch, N. F., Smith, R. G., and Besch, P. K. (1979a). Effect of tetrahydrocannabinol on the hypothalamic-pituitary axis in the ovariectomized rhesus monkey. *Fertil. Steril.* **31**, 335–339.

Smith, R. G., Besch, N. F., Besch, P. K., and Smith, C. G. (1979b). Inhibition of gonadotropin by delta9-tetrahydrocannabinol: mediation by steroid receptors? *Science* **204**, 325–327.

Spears, N., Lopes, F., Stefansdottir, A., Rossi, V., De Felici, M., Anderson, R. A., and Klinger, F. G. (2019). Ovarian damage from chemotherapy and current approaches to its protection. *Hum. Reprod. Update* **25**, 673–693.

Stella, N., Schweitzer, P., and Piomelli, D. (1997). A second endogenous cannabinoid that modulates long-term potentiation. *Nature* **388**, 773–778.

Stocco, C. (2008). Aromatase expression in the ovary: hormonal and molecular regulation. *Steroids* **73**, 473–487.

Sugawara, T., Kiriakidou, M., McAllister, J. M., Kallen, C. B., and Strauss, J. F., 3rd (1997). Multiple steroidogenic factor 1 binding elements in the human steroidogenic acute regulatory protein gene 5′-flanking region are required for maximal promoter activity and cyclic amp responsiveness. *Biochemistry (Mosc)* **36**, 7249–7255.

Sugiura, T., Kondo, S., Sukagawa, A., Nakane, S., Shinoda, A., Itoh, K., Yamashita, A., and Waku, K. (1995). 2-arachidonoylglycerol: a possible endogenous cannabinoid receptor ligand in brain. *Biochem. Biophys. Res. Commun.* **215**, 89–97.

Torrens, A., Ruiz, C. M., Martinez, M. X., Tagne, A. M., Roy, P., Grimes, D., Ahmed, F., Lallai, V., Inshishian, V., and Bautista, M. (2023). Nasal accumulation and metabolism of δ(9)-tetrahydrocannabinol following aerosol ('vaping') administration in an adolescent rat model. *Pharmacol. Res.* **187**, 106600.

Torrens, A., Vozella, V., Huff, H., McNeil, B., Ahmed, F., Ghidini, A., Mahler, S. V., Huestis, M. A., Das, A., and Piomelli, D. (2020). Comparative pharmacokinetics of δ(9)-tetrahydrocannabinol in adolescent and adult male mice. *J. Pharmacol. Exp. Ther.* **374**, 151–160.

van Noord, P. A. H., Boersma, H., Dubas, J. S., te Velde, E. R., and Dorland, M. (1997). Age at natural menopause in a population-based screening cohort: the role of menarche, fecundity, and lifestyle factors. *Fertil. Steril.* **68**, 95–102.

Visser, J. A., and Themmen, A. P. N. (2005). Anti-müllerian hormone and folliculogenesis. *Mol. Cell. Endocrinol.* **234**, 81–86.

Vogel, Z., Barg, J., Levy, R., Saya, D., Heldman, E., and Mechoulam, R. (1993). Anandamide, a brain endogenous compound, interacts specifically with cannabinoid receptors and inhibits adenylate cyclase. *J. Neurochem.* **61**, 352–355.

Wang, J., Paria, B. C., Dey, S. K., and Armant, D. R. (1999). Stage-specific excitation of cannabinoid receptor exhibits differential effects on mouse embryonic development. *Biol. Reprod.* **60**, 839–844.

Wójtowicz, A. K., Kajta, M., and Gregoraszczuk, E. (2007). DDT- and DDE-induced disruption of ovarian steroidogenesis in prepubertal porcine ovarian follicles: a possible interaction with the main steroidogenic enzymes and estrogen receptor beta. *J. Physiol. Pharmacol.* **58**, 873–885.

Zheng, W., Nagaraju, G., Liu, Z., and Liu, K. (2012). Functional roles of the phosphatidylinositol 3-kinases (pi3ks) signaling in the mammalian ovary. *Mol. Cell. Endocrinol.* **356**, 24–30.